© 2014. Published by The Company of Biologists Ltd | Journal of Cell Science (2014) 127, 3916–3927 doi:10.1242/jcs.135269

RESEARCH ARTICLE

Deficits in receptor-mediated endocytosis and recycling in cells from mice with *Gpr107* locus disruption

Guo Ling Zhou*, Soon-Young Na, Rasma Niedra and Brian Seed*

ABSTRACT

GPR107 is a type III integral membrane protein that was initially predicted to be a member of the family of G-protein-coupled receptors. This report shows that deletion of *Gpr107* leads to an embryonic lethal phenotype that is characterized by a reduction in cubilin transcript abundance and a decrease in the representation of multiple genes implicated in the cubilin–megalin endocytic receptor complex (megalin is also known as LRP2). *Gpr107*-null fibroblast cells exhibit reduced transferrin internalization, decreased uptake of low-density lipoprotein (LDL) receptor-related protein-1 (LRP1) cargo and resistance to toxins. Colocalization studies and proteomic analyses suggest that GPR107 associates with clathrin and the retromer protein VPS35 and that GPR107 might be responsible for the return of receptors to the plasma membrane from endocytic compartments. The highly selective deficits observed in *Gpr107*-null cells indicate that GPR107 interacts directly or indirectly with a limited subset of surface receptors.

KEY WORDS: GPR107, Embryonic lethality, Cubilin, Clathrin, Endocytosis

INTRODUCTION

Eukaryotic organisms have evolved highly regulated secretory and endocytic transport pathways to broker the exchange of information and nutrients between extracellular and intracellular compartments. Among the vesicular flows from environment to interior and vice versa, five routes of transport have been especially well studied – (1) retrograde transport from Golgi to endoplasmic reticulum (ER) mediated by coat protein I (COPI), (2) COPII mediated anterograde transport from ER to Golgi, (3) clathrin-mediated endocytosis from plasma membrane to endosomes, (4) retrograde transport from endosomes to the trans-Golgi network (TGN) through clathrin-coated vesicles and (5) caveolar endocytosis to endosomes. Crystallographic structure determination studies have shown that vesicle-coat proteins, including clathrin, COPI and COPII, are conserved from yeast to human and that their assembly mechanisms show noteworthy similarity (Marsh and McMahon, 1999; Pucadyil and Schmid, 2009; Harrison and Kirchhausen, 2010).

Clathrin-mediated vesicular transport, the most highly studied process to date, supports receptor-mediated endocytosis of cargo ligands, such as transferrin, low density lipoprotein, growth factors, antibody complexes and essential factors for cellular proliferation. In this pathway, ligand-bound receptors on the cell surface are entrapped by deformation of plasma membrane domains into coated pits that invaginate, detach from the plasma membrane and undergo a complex, still poorly understood, sorting process (Pucadyil and Schmid, 2009). Clathrin, a key structural element of coated pits, is composed of 190-kDa heavy chains (CHC) and 25-kDa light chains (CLC), which together form three-legged trimmers (called triskelions). The triskelions are assembled into cage-like structures to coat vesicles (Harrison and Kirchhausen, 2010; Marsh and McMahon, 1999). Many of the ancillary molecules that make up the clathrin-coated vesicle have been identified and their structures determined, including a family of adaptor proteins, AP1–AP4, as well as a number of accessory proteins, including AP180/CALM, epsin 1 and endophilin I, that mediate cargo sorting through recognition of specific motifs on receptors (Marsh and McMahon, 1999; Pucadyil and Schmid, 2009).

The participation of GPR107 in the regulation of receptor-mediated endocytosis is the subject of this report. Human *GPR107* was initially identified among cDNAs enriched for expression in lung (Edgar, 2007). The encoded protein was predicted to bear an N-terminal hydrophobic signal peptide, a large extracellular domain and a C-terminal seven transmembrane domain that is characteristic of members of the G-protein-coupled receptor superfamily (Edgar, 2007). GPR107 is highly conserved phylogenetically and counterparts can be found throughout the plant and animal kingdoms, including among mammals, birds, insects, fish, arthropods, dipterans, nematodes, cress, rice and yeast (Edgar, 2007). The protein encoded by the closest paralog in mammals, *Gpr108* (Edgar, 2007), shares 49% identity by amino acid sequence with the protein encoded by *Gpr107* in mice.

In this work, *Gpr107* homozygous null mice have been generated and characterized. Genetic ablation of *Gpr107* results in embryonic lethality between 11.5 and 12.5 days post-coitus. Null embryos exhibit a defect in expression of multiple genes participating in the multi-ligand endocytic receptor pathway that is mediated by cubilin and megalin (also known as LRP2). *Gpr107*-null embryonic fibroblasts exhibit reduced expression of transferrin receptor (TRFC1; also known as TFRC), LRP1 and integrin α5, with corresponding defects in transferrin internalization, LRP1-mediated cargo uptake and fibronectin secretion. GPR107 colocalizes with clathrin and EEA1, and physically interacts with clathrin and VPS35.

RESULTS

Generation of *Gpr107*$^{-/-}$ mice

The *Gpr107* locus in embryonic stem cells was disrupted by using a bacterial artificial chromosome (BAC)-mediated homologous recombination method. The murine gene contains 18 exons, the first 14 of which were excised together with a 2-kb upstream

Center for Computational and Integrative Biology, Massachusetts General Hospital, 185 Cambridge Street, Boston, MA 02114, USA.

*Authors for correspondence (gzhou@ccib.mgh.harvard.edu; bseed@ccib.mgh.harvard.edu)

Received 15 May 2013; Accepted 15 April 2014

Journal of Cell Science

Journal of Cell Science (2014) 127, 3916–3927 doi:10.1242/jcs.135269

region and replaced with a neomycin cassette, as illustrated in Fig. 1A. Correctly targeted clones were identified by multiplex ligation-dependent probe amplification (MLPA) (Langerak et al., 2005) (Fig. 1B) using the probes indicated in Fig. 1A. The neomycin cassette was flanked by R4 integrase attB and attP sites and was deleted by transient expression of R4 integrase in correctly targeted clones. Selected clones were injected into mouse blastocysts to produce chimeric mice. The heterozygous progeny of chimeric animals and homozygous progeny of heterozygous animals were identified using genomic PCR (Fig. 1C) and confirmed using MLPA (data not shown).

Effect of *Gpr107* inactivation on embryonic development

Mice heterozygous for *Gpr107* were mated to generate F2 offspring. From these matings, 164 pups from 27 litters were obtained and genotyped. Of the pups, 106 were heterozygous for *Gpr107* and 58 were wild-type (supplementary material Table S1). No homozygous *Gpr107*-null pups were identified, indicating that the targeted mutation induces an embryonic lethal phenotype. $Gpr107^{+/-}$ mice were physically indistinguishable from their wild-type littermates. At day 10.5, 27 wild-type, 53 heterozygous and 32 homozygous embryos were isolated, consistent with normal Mendelian segregation (supplementary material Table S2). Most of the homozygous embryos were indistinguishable from heterozygous and wild-type embryos at day 10.5, but a small number exhibited reduced size. However, analysis of the smaller embryos did not identify any conspicuous tissue or organ abnormality apart from the size.

Pregnant female mice from heterozygous matings were dissected for isolation of whole embryo and yolk sac at 10.5 days post-coitus. Total RNA was prepared, and reverse transcription and quantitative

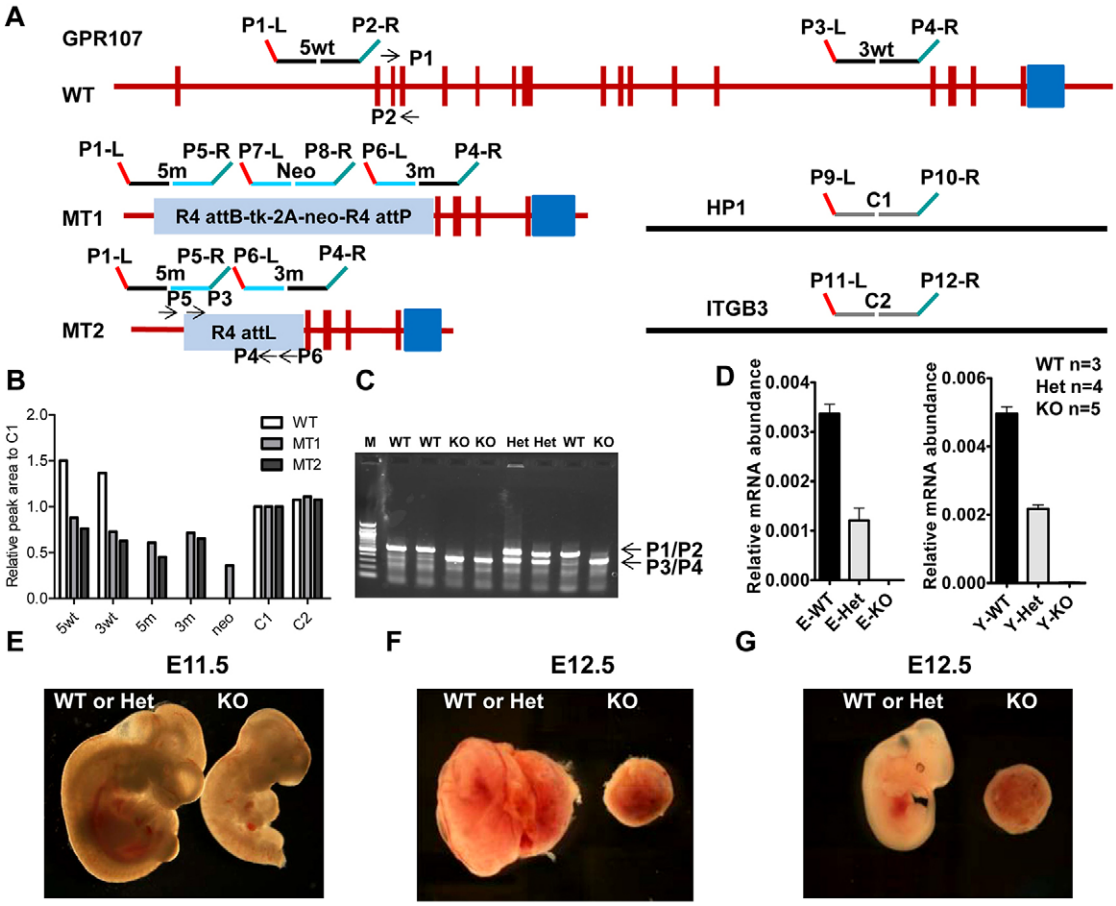

Fig. 1. *Gpr107*-null embryos lose viability around E10.5–11.5. (A) Schematic diagram of the construction of *Gpr107*-knockout mice. The murine *Gpr107* locus contains 17 exons. Using a targeting BAC bearing the selection marker tk-2A-neo flanked by R4 integrase attB and attP sites, exons 1 to 13 were deleted, yielding the MT1 embryonic stem cell line. After expression of R4 integrase in MT1 cells, the resistance elements were removed, as shown in MT2. The probes (shown in supplementary material Table S5) used for MLPA to generate the products 5wt, 3wt, 5m, 3m, neo, C1 and C2 are indicated. The primers P1 and P2, P3 and P4 used for PCR genotyping and P5 and P6 for the R4 deletion test are also shown. The primer suffixes L and R denote left and right, respectively. (B) Representative MLPA fragment analysis of 5wt, 3wt, 5m, 3m, neo, C1, C2 for different target events in wild-type cells, as well as MT1 and MT2 targeted embryonic stem cells. Using *Hp1* (also known as *Cbx5*) (C1) and *Itgb3* (C2) as internal controls to normalize intensities, the 5wt and 3wt signal intensities were observed to be diminished by approximately one half in correctly targeted MT1 cells compared with those in wild-type cells and the copy numbers of 5m, 3m and neo were identified as single copy or greater by analysis of all embryonic stem cell clones exhibiting resistance to G418. In MT2 embryonic stem cells, the neo MLPA signal was not observed following excision by R4 integrase. (C) Individual mouse genotypes obtained by PCR of wild-type (WT), heterozygous (Het) and homozygous knockout (KO) mice are indicated. M, markers. (D) *Gpr107* mRNA abundance in WT, Het and knockout embryos (left) and yolk sac (right). *Gpr107* mRNA was absent from null embryos (E prefix) and yolk sacs (Y prefix) and present in heterozygotes at ~50% of the level found in wild-type embryos. (E) Smaller $Gpr107^{-/-}$ embryos at E11.5. $Gpr107^{-/-}$ embryos that were identified through PCR analysis by using a small piece of yolk sac are smaller than those of heterozygous littermates, although they have normal morphology. (F,G) $Gpr107^{-/-}$ embryos have substantially regressed by E12.5. No $Gpr107^{-/-}$ embryos were identified from normal embryos (represented by the left embryo) in amnion (F) or without amnion and yolk sac (G). $Gpr107^{-/-}$ embryos were identified as regressed (represented by the right embryo) in amnion (F,G) through PCR analysis using a small piece of yolk sac.

Journal of Cell Science (2014) 127, 3916–3927 doi:10.1242/jcs.135269

RT-PCR were performed to analyze *Gpr107* gene expression. The homozygous embryo and yolk-sac tissues contained no *Gpr107* mRNA, and heterozygous embryos showed approximately half the transcript abundance of that found in wild-type embryos and yolk sacs (Fig. 1D). At day 11.5, 18 smaller or markedly deformed nonviable $Gpr107^{-/-}$ embryos were identified among 64 fetuses and were identified as homozygous embryos (supplementary material Table S2); examples are shown in Fig. 1E. At day 12.5, no live $Gpr107^{-/-}$ embryos could be identified from a total of 40 gestations (supplementary material Table S2). However, several embryonic tissues could be isolated from two small implants and were homozygous for *Gpr107* disruption (Fig. 1F,G). These findings indicate that *Gpr107*-null embryos suffer a catastrophic event between 11.5 and 12.5 days post-coitus.

E10.5 *Gpr107*-null embryos exhibit decreased expression of genes associated with the cubilin–megalin multi-ligand endocytic receptor complex

mRNA expression analysis by quantitative sequencing of pooled whole $Gpr107^{-/-}$ and $Gpr107^{+/+}$ embryos at embryonic day (E)10.5 identified a cluster of under-expressed genes in the null cells that encode receptors, ligands and interacting proteins of the cubilin–megalin multi-ligand endocytic receptor complex (Christensen and Birn, 2002), as well as some matrix proteins (supplementary material Table S3). The reduced abundance of cubilin transcripts was validated by quantitative real-time (RT)-PCR in multiple embryos and yolk sacs (supplementary material Fig. S1), as well as by immunofluorescence (data not shown). Cubilin protein expression was lost from $Gpr107^{-/-}$ embryos but not from the visceral yolk sac. Ablation of *Gpr107* reduced the expression of transcripts encoding several ligands of the multi-ligand endocytic receptor complex, including ApoA1, Apo E, Apo M, transferrin and transthyretin, as well as complex-interacting proteins, such as amnionless (Amn) (supplementary material Table S3), that are involved in the maternal–fetal transport of folate and other nutrients (Kozyraki et al., 1999; Kozyraki et al., 2001; Nykjaer et al., 2001; Assémat et al., 2005; Kozyraki and Gofflot, 2007), as well as the transport of lipids and morphogens, such as sonic hedgehog (Shh), and retinoids (supplementary material Table S3), that play crucial roles in normal embryogenesis (Kozyraki et al., 1999; Willnow et al., 1999; Fisher and Howie, 2006; Kozyraki and Gofflot, 2007).

Transferrin transport pathway defects in *Gpr107*-null mouse embryo fibroblasts

Mouse embryonic fibroblast (MEF) cultures were initiated from E10.5 $Gpr107^{-/-}$ embryos and immortalized by using hTERT transduction. To avoid potential confounding effects arising from variation between independently isolated fibroblast lines, a *Gpr107*-reconstituted MEF cell line was created by using retroviral transduction of a *Gpr107* cDNA expression cassette in which the reintroduced *Gpr107* was tagged with a Flag sequence at the C terminus (Fig. 2A). A control cell line that lacked *Gpr107* (knockout) was constructed by transduction of the vector lacking the insert (Fig. 2A). *Gpr107* expression was confirmed by using immunofluorescence and blotting with an antibody against GPR107 (Fig. 2B,C).

Transferrin internalization was tested in the two cell lines through incubation with Alexa-546-conjugated transferrin for

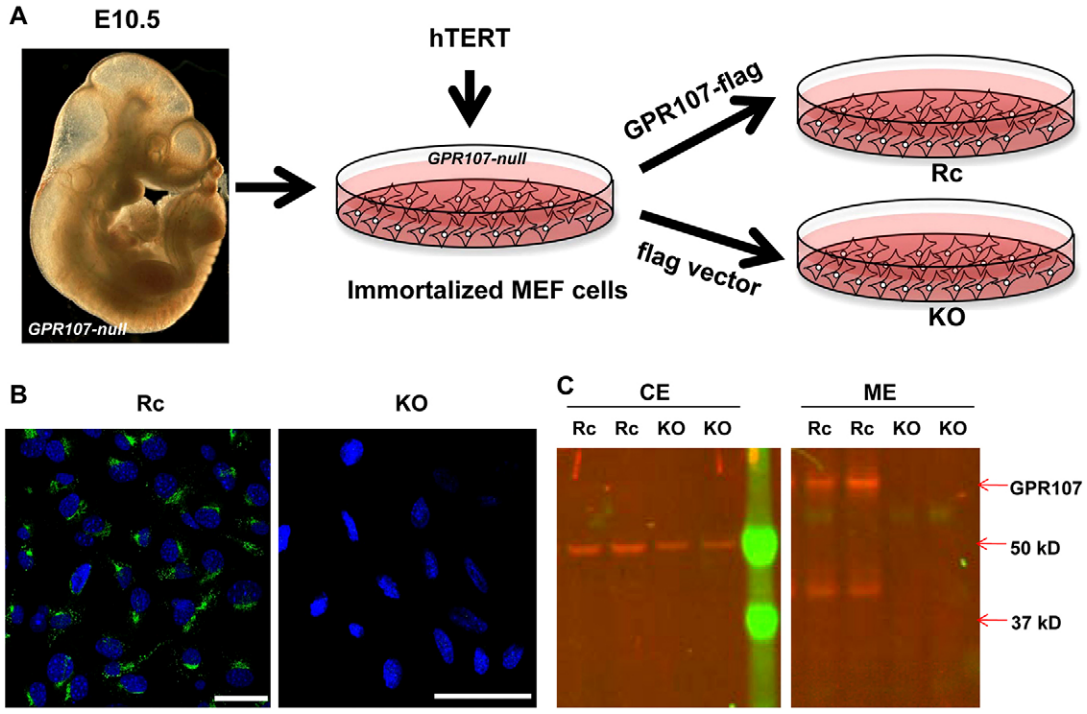

Fig. 2. Generation of *Gpr107*-null cells and *Gpr107*-reconstituted cells from *Gpr107*-null embryonic fibroblast cells. (A) Diagram of process to produce reconstituted and knockout cells. Mouse embryonic fibroblast (MEF) cells were derived from E10.5 *Gpr107*-null embryos and immortalized with hTERT. Flag-tagged *Gpr107* expression vector or empty Flag vectors were introduced into *Gpr107*-null MEF cells by retroviral transduction to create reconstituted (Rc) and knockout (KO) cells. (B,C) GPR107 expression was detected by using immunofluorescence and immunoblotting in reconstituted cells but not in knockout cells. Western blotting detected the expected full-length GPR107 (~66 kDa) and a truncated GPR107 product (~40 kDa) in the membrane fraction but not in the cytoplasmic fraction of reconstituted cells; however, there was a non-specific band in cytoplasmic fraction. CE, cytoplasmic extraction; ME, membrane extraction. Scale bars: 25 μm.

Journal of Cell Science (2014) 127, 3916–3927 doi:10.1242/jcs.135269

different periods of time. Endocytosed transferrin was apparent within 2.5 min in reconstituted cells but did not appear until 20 min in knockout cells (Fig. 3A). When reconstituted and knockout cells that had been labeled with Alexa-546-conjugated transferrin were subsequently chased with unlabeled transferrin, the transferrin signals diminished within 2 h in reconstituted cells but not in knockout cells (Fig. 3B). Transferrin transport was further quantified by measuring the rate of internalization of transferrin and the extent of transferrin receptor recycling using ^{125}I-labeled transferrin. Knockout cells were found to exhibit a higher rate of transferrin internalization and transferrin receptor recycling than reconstituted cells (supplementary material Fig. S2A,B). However, after 50 min, reconstituted cells showed a higher rate of transferrin receptor recycling than knockout cells. Substantially less transferrin was internalized by knockout cells than by reconstituted cells, and less transferrin bound to knockout cells than to reconstituted cells (supplementary material Fig. S2C,D).

Two receptors, TFRC1 and TFRC2, are known to support transferrin-mediated iron transport into cells. Immunoblotting did not reveal any difference in TFRC2 abundance between knockout and reconstituted cells (data not shown). However, TFRC1 mRNA, total protein and surface protein abundance were substantially lower in knockout cells than in reconstituted cells (Fig. 3C,D).

Reconstituted and knockout cells were treated with monensin, chloroquine or bafilomycin A1, agents that increase lysosomal pH through different mechanisms, and surface and total TRFC1 were measured using flow cytometry. Surface TRFC1 proportionately increased by a higher amount in treated knockout cells than in reconstituted cells; however, even after treatment, surface TRFC1 density was higher in reconstituted cells than in knockout cells (Fig. 4B). Bafilomycin A1 in particular produced a substantial increase in surface TRFC1 in both knockout and reconstituted cells (Fig. 4B). Total TRFC1 followed the general pattern of surface TRFC1, albeit with more modest changes. These data are consistent with the view that elevation of the pH of the lysosome or other acidic compartments liberates a greater fraction of internalized receptor in knockout cells than in reconstituted cells. Comparison of the colocalization of TRFC1 and a lysosomotropic dye in the two cell types showed that TRFC1 and lysosomal fluorescence were more highly colocalized in knockout than in reconstituted cells (Fig. 4C).

LRP1-mediated endocytosis is disrupted in E10.5 *Gpr107*-null MEF cells

Cholix toxin is an exotoxin isolated from marine *Vibrio* strains that is structurally related to *Pseudomonas aeruginosa* exotoxin A and has been reported to be endocytosed, like exotoxin A, through an LRP1-mediated process (Jørgensen et al., 2008). Knockout cells that were incubated with 0.5 µg/ml cholix toxin were resistant to its effects, whereas reconstituted cells were sensitive to the toxin and died within 24–48 h (Fig. 5A). After

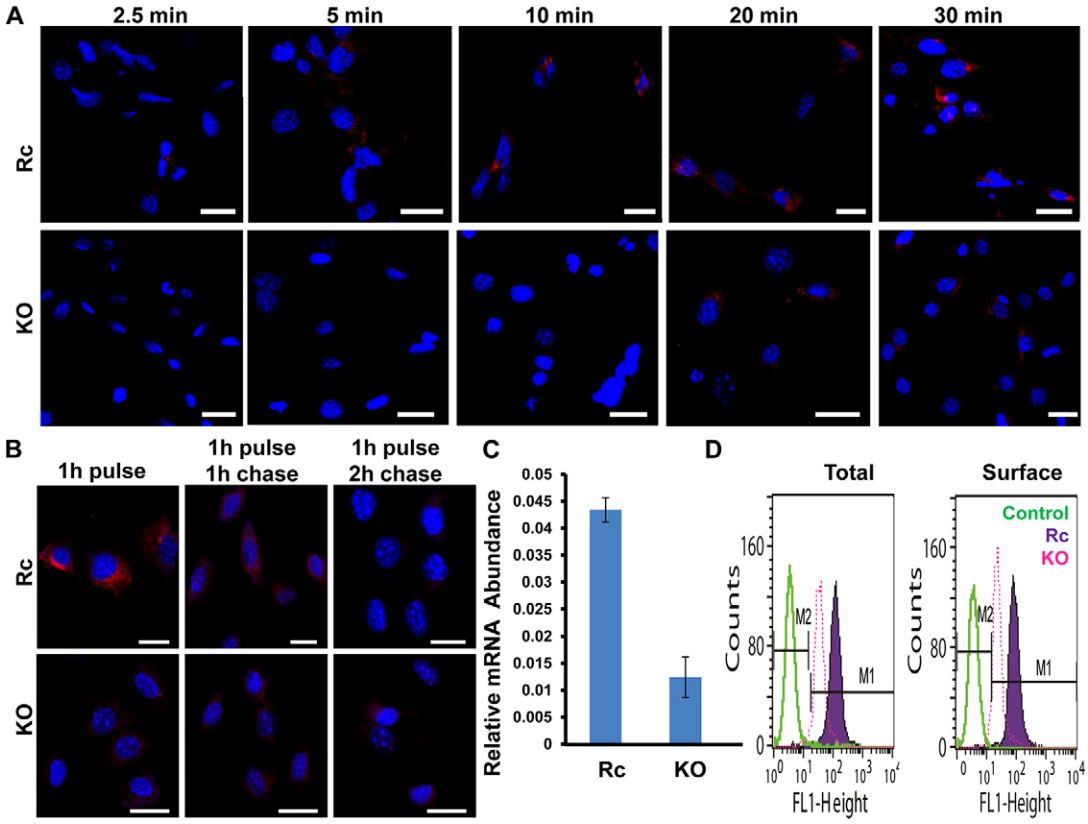

Fig. 3. Transferrin internalization and recycling is attenuated in *Gpr107*-null cells. (A) Timecourse of transferrin uptake in reconstituted and knockout cells. Images recorded at 2.5, 5, 10, 20 and 30 min are shown. Blue, nuclei; red, Alexa-546-conjugated transferrin. (B) After 1-h pulse of Alexa-546-conjugated transferrin, cells were chased with unlabeled transferrin. Transferrin abundances (red) in reconstituted (Rc) and knockout (KO) cells were assessed following 0, 1- and 2-h chases. (C) Transferrin receptor 1 (*Trfc1*) mRNA was measured by using reverse transcription quantitative RT-PCR. Means±s.d. are shown. TRFC1 protein level was measured by using flow cytometry analysis. Green, isotype control; blue, reconstituted cells; pink, knockout cells. *Trfc1* mRNA (C), and total and surface TRFC1 protein (D) were decreased in null MEF cells. M1, negatively staining cells; M2, positively staining cells. Scale bars: 25 µm.

Journal of Cell Science (2014) 127, 3916–3927 doi:10.1242/jcs.135269

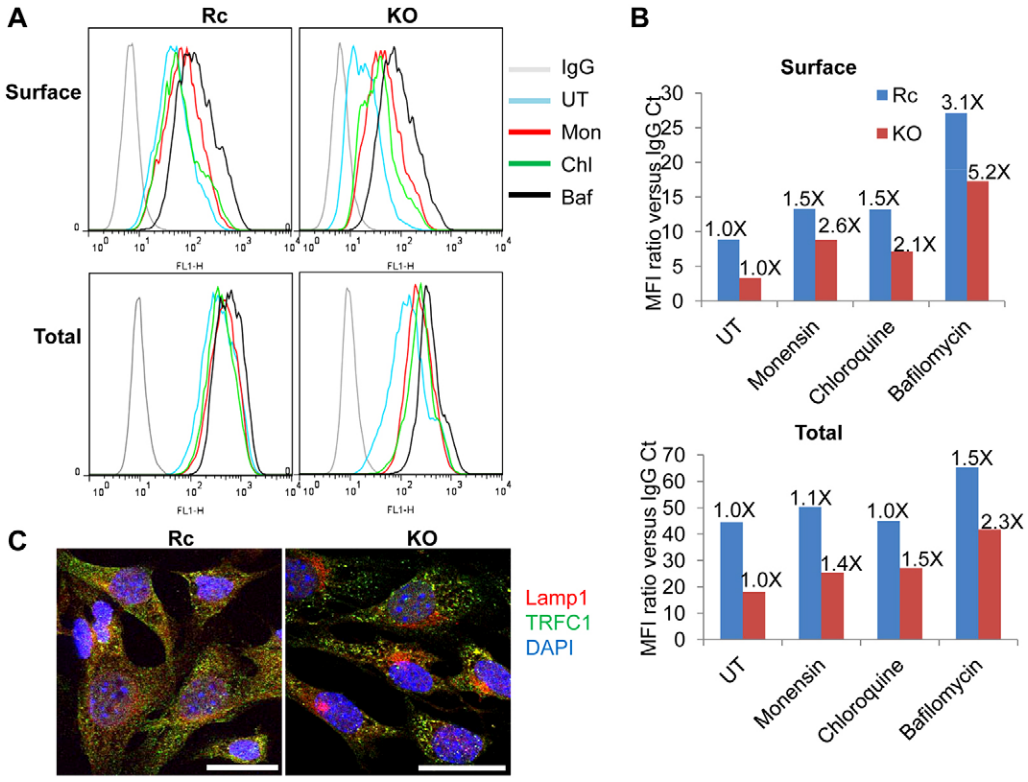

Fig. 4. Exposure to agents elevating vesicular pH exposes a greater proportion of surface TRFC1 on *Gpr107*-null cells than reconstituted cells. (A) Surface and total TRFC1 were measured by cytometry analysis relative to isotype-matched control antibody staining (IgG, gray) on reconstituted (Rc) and knockout (KO) cells following treatment with agents that elevate vesicular pH compared with untreated cells (UT, blue). The agents used include monensin (Mon, red), chloroquine (Chl, green) and bafilomycin A1 (Baf, black). (B) Mean fluorescence intensity (MFI) ratio between TRFC1 antibody staining and control IgG staining is shown for reconstituted and knockout cells. The numbers above the bars represent the fold changes relative to the untreated cell line control. (C) Immunofluorescence staining of TRFC1 (green) and LAMP1 (Red) in reconstituted and knockout cells. DAPI, blue. Scale bars: 25 μm.

72 h of treatment with the toxin, a tetrazolium reduction (MTS) assay showed that electron transport in reconstituted cells was substantially impaired, yielding a density of formazan that was approximately one third of that of knockout cells (Fig. 5A).

LRP1, a multi-cargo receptor megalin homolog, comprises a 515-kDa heavy chain containing four clusters of ligand-binding domains and a non-covalently associated 85-kDa light chain that contains a trans-membrane and cytoplasmic domain, which together are responsible for the internalization of diverse ligands (Herz and Strickland, 2001). An LRP1 functional deficit that was attributable to *Gpr107* inactivation was established by analysis of the rate of internalization of Alexa-488-conjugated LDL. After 1 h of incubation with conjugated LDL, knockout cells were found to internalize less LDL than reconstituted cells (Fig. 5B). Quantitative RT-PCR and immunoblotting studies showed that *Lrp1* mRNA, as well as total and surface LRP1 protein, were significantly decreased in knockout cells compared with reconstituted cells, but the ratio of precursor to mature LRP1 was the same in both cell types (Fig. 5C,D; supplementary material Fig. S3). Surface LRP1 was assessed by vectorial labeling using a water-soluble biotin N-hydroxysulfosuccinimide ester followed by blot detection. Flow cytometry analysis showed that agents that increased acidic compartment pH increased surface LRP1 more prominently in knockout cells than that in reconstituted cells (supplementary material Fig. S4A).

Integrin-α5-mediated fibronectin-1 secretion is compromised in E10.5 *Gpr107*-null MEF cells

Quantitative proteomic analysis of secreted proteins was performed by using differential stable isotope labeling. Reconstituted and knockout cells were incubated in medium containing arginine and lysine that were deuterated or unlabeled, respectively, and the supernatant was collected and concentrated. The secreted protein mixtures were fractionated by using gel electrophoresis. A highly expressed protein was identified from reconstituted cells (Fig. 6A) but not knockout cells. Digestion and mass spectrometry analysis showed constituent peptides of fibronectin-1, and quantitative analysis showed that fibronectin expression was three- to fourfold higher in reconstituted cells compared with that of null cells (Fig. 6B,C). The abundance of mRNA encoding integrin α5 (*Itga5*) and integrin β1 (*Itgb1*), which comprise the fibronectin-1 receptor α and β chains, respectively, was analyzed by using quantitative RT-PCR, and the *Itga5* mRNA level was found to be reduced in the *Gpr107*-null cells whereas no significant change was found for *Itgb1* (Fig. 6D). Flow cytometry analyses showed that both the integrin α5 cell surface density and the combined intracellular and plasma membrane density (total integrin abundance) were significantly lower in knockout cells than reconstituted cells, suggesting that the reduced fibronectin-1 secretion could be related to the decreased expression of fibronectin receptor in knockout cells (Fig. 6E). Flow cytometric analysis also showed that agents that elevated acidic compartment pH enhanced the integrin α5 surface expression on knockout cells to a greater degree than that observed with reconstituted cells (supplementary material Fig. S4B).

GPR107 interacts with clathrin heavy chain and VPS35

Immunoprecipitation of tagged GPR107 or the tag alone was performed from lysates of reconstituted and knockout MEF cells, respectively. Mass spectrometry analysis of the peptides liberated from the co-precipitated proteins showed a prominent over-representation of peptides from proteins involved in clathrin-mediated endocytosis and retrograde transport from the TGN to endosomes (supplementary material Table S4). Clathrin (CLTC) and vacuolar protein sorting 35 (VPS35) were the top putative binding partners of GPR107 from these pathways. To validate the

Journal of Cell Science (2014) 127, 3916–3927 doi:10.1242/jcs.135269

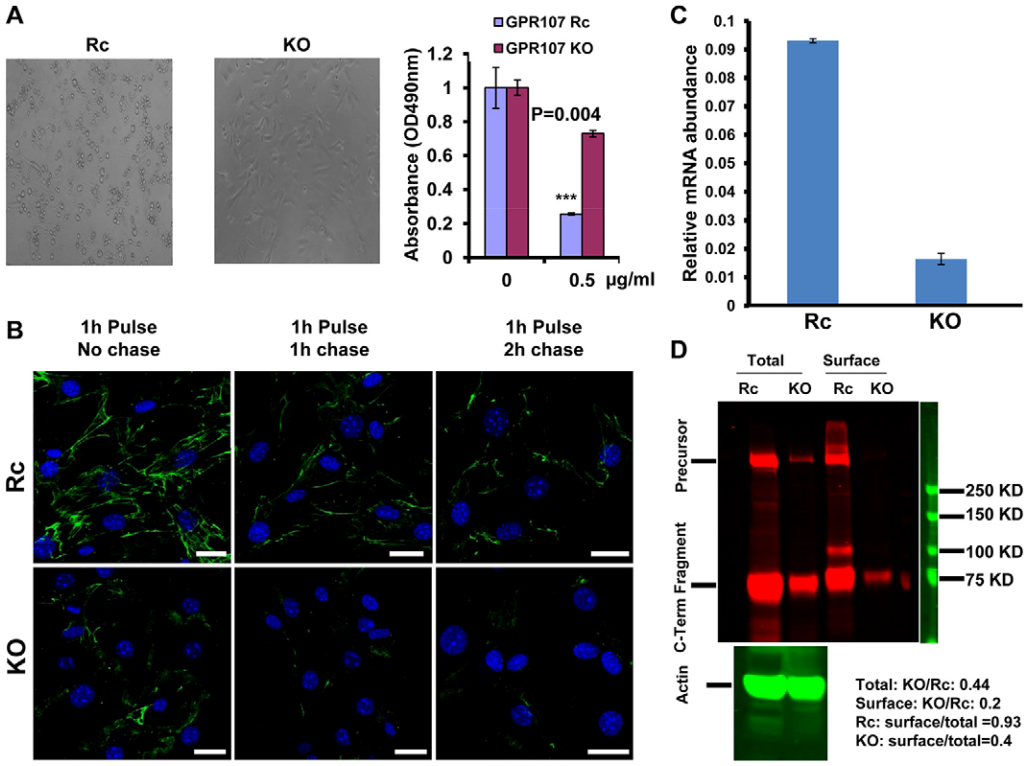

Fig. 5. *Gpr107*-null cells are resistant to LRP1-dependent toxin cytotoxicity and internalize LDL poorly. (A) *Gpr107*-reconstituted (Rc) cells were sensitive to 0.5 µg/ml cholix toxin but knockout (KO) cells were resistant. Cholix toxin shows greater cytotoxicity to *Gpr107*-reconstituted cells than knockout cells within 72 h when evaluated by using an MTS assay. Means±s.d. are shown, $n=3$, ***$P=0.004$. (B) *Gpr107*-null MEF cells exhibit defects in LDL loading and exocytosis. After a 1-h pulse of Alexa-488-conjugated LDL, reconstituted and knockout cells were fed with fresh medium and bound LDL (green) was assessed after incubation for 0, 1, 2 and 5 h. Scale bars: 25 µm. (C) *Lrp1* mRNA is reduced in *Gpr107*-knockout cells compared with that of reconstituted cells. Means±s.d. are shown, $n=3$. (D) LRP1 abundance on the cell surface and in intracellular compartments is lower in *Gpr107*-null (KO) cells compared with reconstituted cells. Surface proteins were isolated following sulfo-NHS-SS-biotin labeling by streptavidin bead adsorption. Total cell lysate and surface proteins were separated in 4–12% SDS-PAGE gels and blotted with an antibody against LRP1. The blot was quantified by ratiometric infrared fluorescence imaging using the actin signal intensity to normalize the data. Abundance ratios derived from analysis of the two cell lines are shown below the image.

interaction between GPR107 and CLTC or VPS35, tagged GPR107 was expressed in the human cell line 293ETN and subjected to immunoprecipitation followed by immunoblot analysis using antibodies against CLTC or VPS35. A specific interaction was readily detected with CLTC and VPS35 proteins (Fig. 7A). A reciprocal co-immunoprecipitation reaction using an antibody against CLTC and tagged VPS35 followed by blotting for GPR107 also demonstrated an association between these proteins (Fig. 7B). A similar experiment was performed in reconstituted and knockout MEF cells in which Flag-tagged GPR107 was immunoprecipitated and subjected to blot analysis using antibodies against CLTC and VPS35, yielding similar results (Fig. 7C).

GPR107 colocalizes with a fraction of clathrin-containing and early endosomal vesicular structures

GPR107 localization was studied by using confocal microscopy analysis of cells that expressed GPR107 fused with green fluorescent protein (GFP) or by similar analysis of reconstituted cells following staining with an antibody against GPR107. A high degree of colocalization of GPR107 with a discrete fraction of clathrin-associated vesicular structures in a perinuclear localization was observed (Fig. 7D). A similar, but slightly less concordant co-staining was seen with the early endosome marker EEA1, whereas the late endosome markers RAB9 and the mannose-6-phosphate receptor (also known as IGF2R), and the lysosome marker LysoTracker showed very limited colocalization (Fig. 7D).

N- and C-terminal domains of GPR107 are important for interaction with clathrin

In order to map which domains on GPR107 mediate interaction with CLTC, three mutants, m1, m2 and m3, were constructed (shown in Fig. 8A). GPR107 has a predicted extracellular N-terminal domain, three intracellular loops and a short C-terminal domain. The N-terminal and C-terminal domains were truncated to give mutants m1 and m3, respectively. Loop 3 was replaced by a substitute sequence in mutant m2 (Fig. 8A). The intracellular distribution of the mutants fused to GFP was characterized in HeLa cells (Fig. 8B). Mutants m1 and m2 retained a similar distribution to wild type, but m3 was seen to be dispersed on vesicles located throughout the cytoplasm, suggesting that the deleted C-terminal domain provides signals for restriction to a subset of vesicles. The fluorescence intensity of the m3–GFP fusion protein in the transfected cells was conspicuously dim (data not shown). Neither m1or m3 could be co-immunoprecipitated with CLTC, unlike mutant m2 (Fig. 8C). The m3 protein exhibited poor expression in transfected 293ETN cells, consistent with the microscopy analyses (Fig. 8C).

DISCUSSION

In this study, the *Gpr107* locus was disrupted by using a BAC-mediated gene targeting strategy. *Gpr107* ablation had profound

Journal of Cell Science (2014) 127, 3916–3927 doi:10.1242/jcs.135269

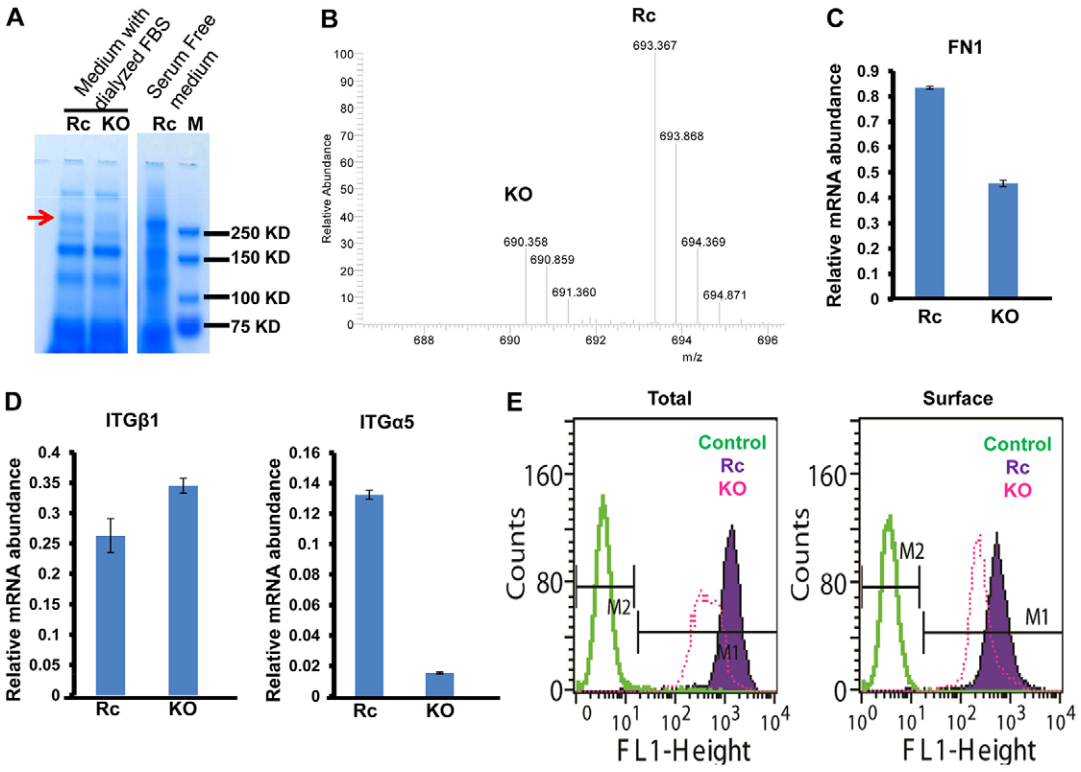

Fig. 6. Fibronectin-1 secretion is reduced in *Gpr107*-knockout MEF cells. (A) One major species (indicated by red arrow) was reduced in knockout (KO) culture medium compared with reconstituted (Rc) culture medium. (B) Characteristic fibronectin-1 peptides isolated from reconstituted cells and identified by mass spectrometry are threefold more abundant than those isolated from null cells. The proteins from reconstituted and knockout cells were labeled by heavy (^{13}C, ^{15}N) and light stable isotopes (^{12}C, ^{14}N), respectively, and distinguished by molecular mass. (C) The mRNA level of fibronectin-1 (*Fn1*) is decreased in knockout cells. (D) Abundance of fibronectin-1 receptor integrin α5 (ITGα5) transcripts is decreased in knockout cells, whereas abundance of integrin β1 transcripts is similar between the two cell types (ITGβ1). (E) Both surface and total integrin α5 are reduced in knockout cells compared with that of reconstituted cells. Green, isotype control; blue, reconstituted cells; pink, knockout cells. M1, negatively staining cells; M2, positively staining cells.

consequences for embryogenesis, resulting in a loss of viability between 11.5 and 12.5 days post-coitus. Transcript abundance profiling through sequencing identified selective defects in cubilin–megalin-related trafficking, which appeared to contribute to or account for the observed embryonic lethality. Cubilin gene expression was prominently diminished at E10.5, the start of the critical period for *Gpr107* homozygote survival.

Previous data have shown that the multi-ligand endocytic receptors cubilin and megalin exert their roles in the visceral epithelial cells of the embryonic yolk sac, intestine, kidney and thyroid gland and participate in the transportation of vitamins B12 and D3, lipid-binding proteins, poorly water soluble hormones and their binding proteins, mineral-binding proteins and a variety of heterogeneous ligands (Kaseda et al., 2011; Kozyraki et al., 1999; Kozyraki et al., 2001; Nykjaer et al., 2001; Christensen and Birn, 2002; Christensen and Verroust, 2002; Fisher and Howie, 2006; Kozyraki and Gofflot, 2007). Because cubilin mediates nutrient transport from the maternal to the fetal circulation, the loss or partial incapacitation of cubilin and megalin function could be expected to jeopardize fetal development. In addition, transcripts encoding collagen subtypes and fibrinogen were found at reduced levels in homozygote embryos. Because fibrinogen stabilizes placental–maternal attachment during embryonic development (Iwaki et al., 2002), mechanical factors might have additionally contributed to the observed embryonic lethality. Embryonic defects in matrix assembly might also be implicated in the organismic phenotype in light of the diminished expression of fibronectin-1 in *Gpr107*-null mouse fibroblasts cells. The fibronectin synthesis defect, in turn, might be related to diminished expression of the fibronectin receptor subunit integrin α5, which participates in matrix deposition and remodeling (Arai and Nishiyama, 2007; Goossens et al., 2009).

To better understand the function of *Gpr107*, reconstituted and null cell lines were established from embryonic fibroblast cells that had been derived from null mouse embryos. Transport defects were found in *Gpr107*-null cells that involved a subset of plasma membrane receptors that undergo clathrin-coated vesicular recycling, represented by TRFC1, LRP1 and integrin α5. A substantial decrease in cargo internalization by *Gpr107*-null cells was observed that could be explained by the decreased density of surface receptors on *Gpr107*-null cells.

GPR107 co-immunoprecipitated with clathrin and VPS35, and confocal microscopy indicated that GPR107 colocalizes with a subset of vesicles containing clathrin, as well as a subset of vesicles containing the early endosome marker EEA1. Little localization to vesicular structures that were associated with late endosome markers or the lysosome was observed. The finding that only a subset of clathrin-associated or EEA1-associated vesicles contains GPR107 is consistent with the observation that only a limited set of receptors appeared to be affected by disruption of the gene.

Multiple adaptor proteins have been defined that facilitate clathrin-dependent endocytosis in the early stage of vesicle

Journal of Cell Science (2014) 127, 3916–3927 doi:10.1242/jcs.135269

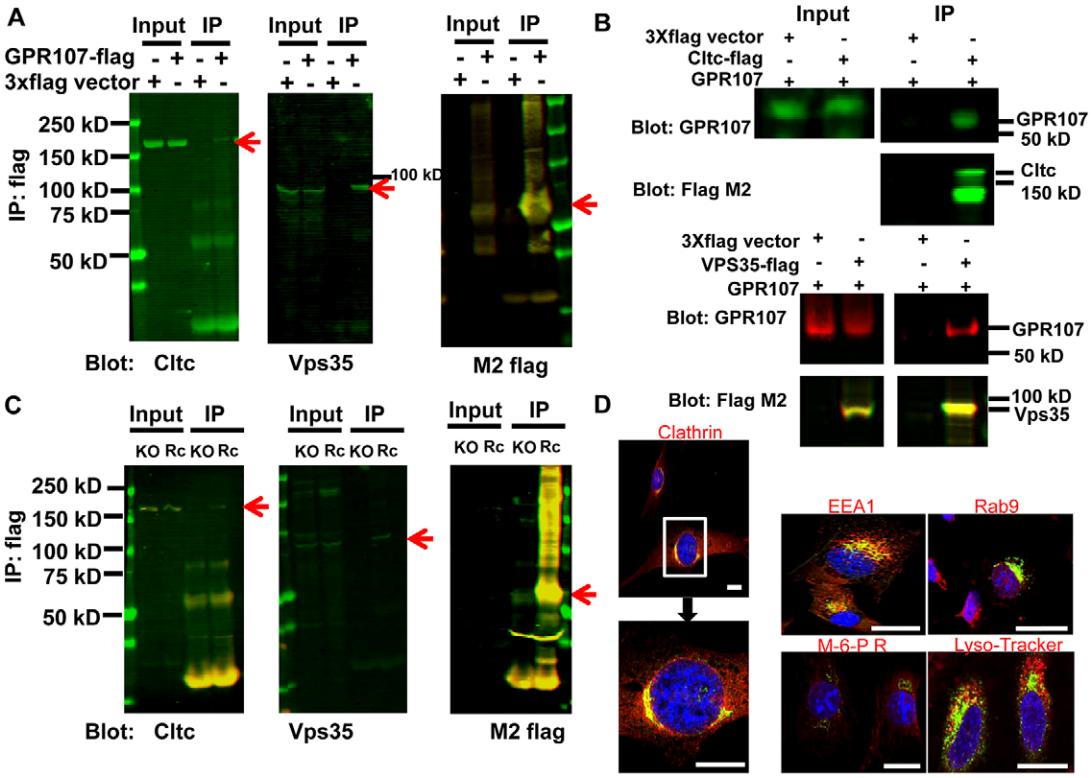

Fig. 7. GPR107 interacts with CLTC and VPS35. (A) Co-immunoprecipitation experiment in 293ETN cells. *Gpr107*-Flag expression vector or Flag empty vector was transfected into 293ETN cells, and cell lysates were immunoprecipitated (IP) using anti-Flag beads. The immunoprecipitates were examined by immunoblotting using antibodies recognizing Flag, CLTC or VPS35. Input represents 10% of the cell lysates used in the co-immunoprecipitation experiment. (B) Verification of GPR107 interaction with CLTC by reciprocal co-immunoprecipitation in 293ETN cells. CLTC-Flag, VPS35-Flag or Flag empty vector and *Gpr107* vector were co-transfected into 293ETN cells as indicated, and cell lysates were immunoprecipitated using anti-Flag beads. The immunoprecipitates were examined by immunoblotting using anti-Flag or anti-GPR107 antibody. CLTC-Flag can be detected by an antibody against Flag after anti-Flag bead enrichment but not before enrichment. (C) Co-immunoprecipitation experiment in reconstituted (Rc) and knockout (KO) MEF cells. The GPR107 band is not visible in the input sample owing to low concentration in the total cell lysate but could be detected in the membrane fraction using a high sample load (shown in Fig. 2). (D) GPR107 colocalizes with a fraction of clathrin and EEA1 vesicles. Reconstituted MEF cells were stained with antibodies against clathrin, the early endosome marker EEA1 or the late endosome marker mannose-6-phosphate receptor (M-6-P R, red), as well as an antibody against GPR107 (green). The late endosome marker RAB9 and LysoTracker (red) were also visualized in HeLa cells expressing GPR107 (green). The white box in the Clathrin staining image highlights the area shown in the inset image. Red arrows in A and C indicate detected protein bands. Scale bars: 25 μm.

formation and that recognize specific motifs, such as NPxY or YxxΦ on receptors, bridging cargo-laden receptors and clathrin (Wolfe and Trejo, 2007). The adapter proteins differ from GPR107 in their fundamental structural organization because they lack a transmembrane topology. However, like the ER retention receptor (KDELR1), which recognizes the KDEL motif (Lewis and Pelham, 1990; Pelham, 1991; Majoul et al., 2001), GPR107 has a seven transmembrane organization and is nearly exclusively expressed in vesicular structures within the cell. Also like the KDEL receptor, GPR107 is phylogenetically highly conserved and appears to support a fundamental eukaryotic process. Although such a function has not been attributed to the KDEL receptor to date, GPR107 might have a signaling role that instructs the cell to perform endocytic processing steps that are important for the subset of receptors that depend on its presence for sorting into different compartments. *Gpr107*-null embryos showed reduced transcript abundance for large multi-ligand receptors and their cargo. These receptors might undergo a specialized sorting pathway related to the transport functions that they support.

Some receptors that have been traditionally considered to ferry a single type of cargo were also found to be influenced by ablation of *Gpr107*. A striking discrimination was found between the behaviors of transferrin receptors type 1 and type 2 where the former was dependent on a GPR107-mediated process but the latter was unaffected. Similarly, integrin α5 expression was reduced in the absence of GPR107, whereas integrin β1 expression was unaffected.

Although the decreased surface density of affected receptors in *Gpr107*-null fibroblasts is consistent with a lesion in pathways transporting proteins to the plasma membrane, clathrin-mediated retrograde transport from endosome to TGN might also be implicated in the reduction of receptor surface density. Two proteins, CLTC and retromer protein VPS35, were identified among proteins that co-immunoprecipitated with GPR107. The retromer complex, which includes VPS26, VPS29, VPS35, SNX1 and possibly SNX2, SNX5 and SNX6 in mammals, plays an important role in recycling transmembrane receptors from endosomes to TGN (Wassmer et al., 2007; Pfeffer, 2001; Seaman, 2005). The association between GPR107 and clathrin and VPS35 might indicate that GPR107 retrieves receptors from a compartment containing these proteins.

Recently, a forward genetic screen in haploid embryonic stem cells has identified *Gpr107* as a crucial determinant of ricin

Journal of Cell Science (2014) 127, 3916–3927 doi:10.1242/jcs.135269

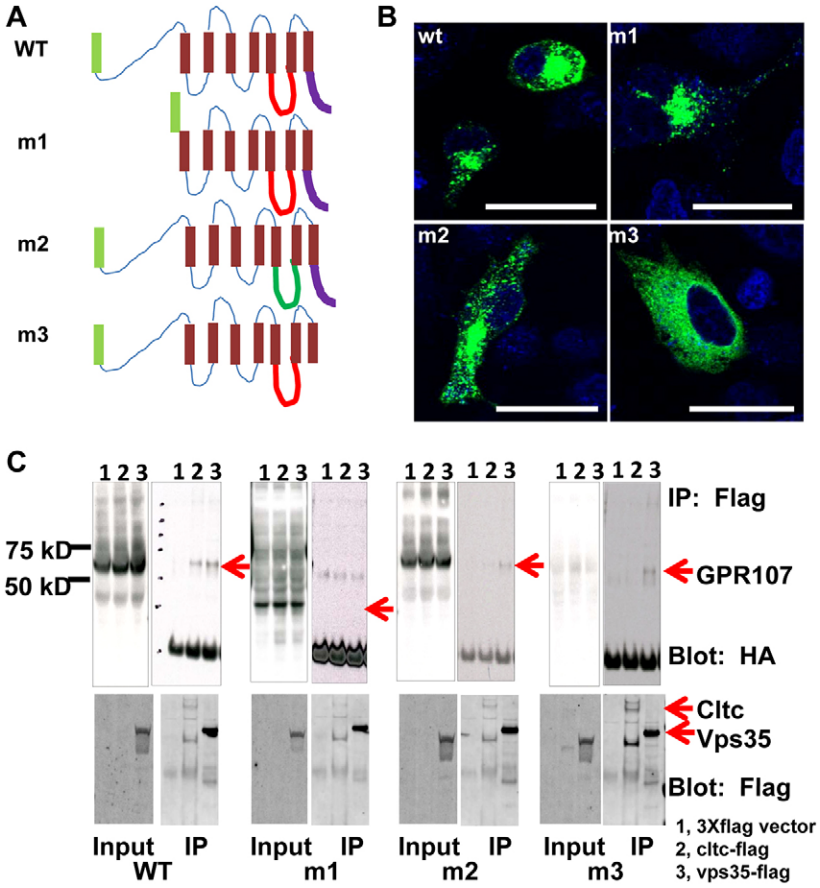

Fig. 8. Mapping the domain of GPR107 that binds to CLTC. (A) Three mutants of GPR107: m1, m2 and m3, were constructed with a hemagglutinin (HA) tag. m1 has a deletion in the N-terminal domain but retains the signal peptide (green box), m2 has a replacement of the loop 3 sequence EASATDGKAAINLAK (red loop) with GGGSGGGSGGGSEGG (green loop) and m3 has a deletion in the C-terminal domain (dark blue). Localization of GPR107 and the three mutants was visualized by fusion with GFP. (B) Deletion of the GPR107 C-terminal domain alters localization in cells. (C) Binding to CLTC is lost upon deletion of either the N-terminal or C-terminal domain, but binding to VPS35 is only affected by deletion of the N-terminal domain. Co-immunoprecipitation was performed in 293ETN cells by co-expressing HA-tagged wild-type (WT) GPR107 or three mutants with Flag-tagged control (3×Flag vector), CLTC or VPS35. IP, immunoprecipitation. Red arrows indicate detected protein bands.

sensitivity (Elling et al., 2011). Lesions in *Gpr107* were the most frequently identified mutations among independently isolated ricin-resistant clones (Elling et al., 2011). Because ricin is a galactose-binding lectin, it has been commonly supposed that the toxin has no specific proteinaceous receptor, a view that is supported by the paucity of plasma membrane proteins identified in the ricin-resistance screen (Elling et al., 2011). However, the existence of a specific receptor that cannot be mutated without compromising cellular viability cannot be excluded. The finding that *Gpr107* ablation confers protection supports the view that the pathway *Gpr107* subserves might have particular importance for toxins that undergo retrograde transport to the ER, such as cholix toxin, shiga toxin and ricin. The receptors that can initiate retrograde transport might constitute a distinct subset, possibly as a consequence of their cargo delivery mechanisms, that highly overlap with the client receptors of GPR107.

MATERIALS AND METHODS

Animals and reagents

Mouse studies were conducted under protocols approved by the institutional animal care and usage committee of Massachusetts General Hospital. Alexa-546-conjugated transferrin, Alexa-488-conjugated LDL, LysoTracker and MitoTracker were obtained from Life Technologies.

Plasmid constructions

Gpr107 cDNA without the Flag tag was inserted into expression vector pEAK15. *Gpr107*, *Vps35* and *Cltc* cDNAs with Flag tag were inserted into the expression vector pCMV-3×Flag. *Gpr107* and its three mutants were also inserted into the expression vector pCMV-3×HA. *Gpr107* with Strep II and Flag tags were inserted into the pZome viral vector.

Antibodies

Anti-GPR107 peptide antibodies were produced by immunizing rabbits with KLH-peptide conjugates. The following sources for commercially available antibodies were used: anti-cubilin (Santa Cruz Biotechnology; sc-23644); anti-clathrin (heavy chain; Santa Cruz Biotechnology, sc-271178; Abcam, ab2731); anti-TFRC1 (Abcam; ab633335); anti-TFRC2 (Abcam; ab83810); anti-LRP1-heavy-chain (Sigma-Aldrich; L2420); anti-LRP1-light-chain (Abcam; ab28320); anti-integrin-α5 (Abcam; ab25076); anti-VPS35 (Abcam; ab10099); anti-M-6-P-receptor (Abcam; ab2733); anti-RAB9 (ab2810); anti-PDI (Abcam; ab2792); anti-EEA1 (Sigma-Aldrich; E7659); anti-Flag M2 (Sigma-Aldrich; F1804).

Generation of *Gpr107*-null mice

The targeting BAC was constructed by using homologous recombination between a small targeting vector and BAC clone RP23-361I14 in *Escherichia coli*, following general procedures that have been described elsewhere (Yang and Seed, 2003). The targeting BAC was linearized at a single PI-*Sce*I site and electroporated into mouse W4/129S6 embryonic stem cells (Taconic). Clones that were resistant to G418 (200 μg/ml) were screened using MLPA with multiplex MLPA probes (supplementary material Table S5). Six positive clones were identified out of 96 tested. Two lines, 5G06 and 5H02, were transfected with an R4 integrase expression plasmid to delete the TK-neo cassette. The resultant ganciclovir (GCV)-resistant cells were tested by using PCR analysis with a pair of primers (P5, P6; shown in supplementary material Table S5). PCR products were sequenced to confirm the deletion events. Removal of the neomycin phosphotransferase coding sequences was affirmed by MLPA. Chimeric mice were generated by injecting C57BL/6 blastocysts with 8–12 cells that had been derived from the engineered embryonic stem lines. Seven male chimeric animals were produced, two of which transmitted the *Gpr107* mutation into the next generation. Heterozygous mice were maintained, and mating was initiated to generate homozygous mutants.

Journal of Cell Science (2014) 127, 3916–3927 doi:10.1242/jcs.135269

Derivation of *Gpr107*-null E10.5 MEF cells and establishment of reconstituted GPR107 MEF cells

Primary embryonic fibroblasts were derived from 10.5-day-old fetuses and cultured in Iscove's modified Dulbecco's medium (IMDM) with 10% iron-supplemented calf serum, glutamine, non-essential amino acids and 10 µg/ml gentamicin. hTERT-immortalized *Gpr107*-null MEF cells were generated by transduction with hTERT virus (Applied Biological Materials). Two subsequent MEF cell lines, *Gpr107* Rc (reconstituted cells) and *Gpr107* knockout (vector control), were established through stable expression of *Gpr107* cDNA fused with Flag-tag-coding sequences or with empty Flag vector, respectively, in *Gpr107*-null MEF cells.

RNA-Seq and data analysis

Total RNA was extracted from E10.5 whole embryos using Trizol (Invitrogen) and purified using RNeasy columns (Qiagen). The sequencing library was prepared according to the manufacturer's instructions using an mRNA sequencing kit (Illumina). Sequencing was performed in the Genomics core of Tufts University Medical Center. A list of mouse mRNAs was downloaded from the UCSC Genome browser database (http://hgdownload.cse.ucsc.edu/downloads.html#mouse). Sequences were matched to the mRNA database using either Bowtie or BLAST. For each read, only the best match was kept. The number of reads that matched each mRNA was then counted. Assuming the total number of transcripts in each cell is on the order of 500,000 copies (Carter et al., 2005) and the read counts are proportional to the transcript copy number and the length of the transcripts, the number of reads was then converted to an estimated transcript copy number.

RNA preparation and quantitative RT-PCR

Total RNA was extracted and purified using an RNeasy kit (Qiagen) from MEF cells or from embryos or yolk sacs dissected from maternal uterus. All primers except those specialized for *Gpr107* were selected from PrimerBank (http://pga.mgh.harvard.edu/primerbank/) and are detailed in supplementary material Table S5. Reverse transcription and quantitative RT-PCR mixes were prepared with SuperScript II Reverse Transcriptase (Invitrogen) and iQ™ SYBR® Green Supermix (Bio-Rad) and performed in triplicate on a Bio-Rad iQ5 instrument. Primer sequences are listed in supplementary material Table S6.

Immunofluorescence

Embryonic tissue sections were prepared by sectioning frozen tissues in optimal cutting temperature (OCT) compound. For microscopy of cells in culture, 10,000 cells were seeded onto coverslips in a 12-well plate. Tissue sections or cells on coverslips were fixed in 2% paraformaldehyde for 15 min and permeabilized in 0.5% SDS in PBS for 4 min. Cells were fixed in fixation buffer (BD Biosciences) for 15 min and permeabilized with 0.3% Triton X-100 in PBS with 5% bovine serum albumin (BSA) for 10 min. Nonspecific fluorescence was blocked by using blocking solution (BD Biosciences) supplemented with 1% goat serum. Tissue sections or coverslips were incubated overnight at 4℃ with a rabbit polyclonal antibody against cubilin. Staining was visualized using a secondary Alexa-546-conjugated anti-rabbit IgG (1 in 200; Invitrogen). DNA was counterstained with Hoechst 33258 before slides were mounted. Cells were visualized by using a fluorescent microscope with a 63× oil-immersion objective.

MEF cells grown on glass coverslips were washed with PBS and fixed for 10 min with 4% (w/v) paraformaldehyde in PBS at room temperature or with 100% methanol at −20℃ for 1 h. Cells were rinsed five times with PBS. The cells were permeabilized with 0.3% Triton X-100 prepared in blocking solution (PBS containing 3% BSA and 5% v/v goat serum) for 30 min. Cells were stained with the indicated antibodies for 2 h at room temperature, followed by incubation with fluorescence-labeled secondary antibodies. Imaging was performed on a Leica SP5 AOBS confocal microscope equipped with argon-krypton, and 543/594 nm helium-neon lasers. Images were acquired using a 40× or 63× objective and the appropriate filter combination.

Transferrin internalization and recycling in MEF cells

Reconstituted and knockout cells were seeded into 12-well plates with coverslips and incubated in medium overnight. The next day, the cells were washed with serum-free medium three times and incubated with serum-free medium for 2 h. The medium was replaced with fresh serum-free medium containing Alexa-546-conjugated human transferrin. For transferrin internalization, the reaction was stopped by washing with PBS at different times and the cells were fixed in fixation buffer (BD Biosciences). Subsequently GPR107 protein was localized by using immunostaining and visualized as described above for immunofluorescence. For transferrin recycling, cells were exposed to transferrin for 1 h. After washing with fresh serum-free medium, the culture was fed with fresh medium for transferrin chase. Cells were fixed at different times and observed by using confocal microscopy.

Measurement of kinetics of transferrin internalization

Reconstituted and knockout cells (3×10^5) were plated on a 6-well plate one day before the experiment to allow for ~80–90% confluence on the day of experiment. Triplicate wells for each condition were prepared, plus one additional well for competition. On the day of the experiment, the cells were washed with serum-free IMDM and incubated in serum-free medium with 0.2% BSA for 1 h at 37℃. The cells were then exposed to 1 ml serum-free medium with 0.2% BSA containing 2 µg/ml ^{125}I-labeled human transferrin (500 ng/ml ^{125}I-transferrin (PerkinElmer) and 1500 ng/ml human transferrin) to triplicate wells and a 500-fold excess of unlabeled transferrin was added to the competition well. Cells were incubated at 37℃, removed at the indicated time points (2, 5, 10, 30, 60 min), placed on ice, washed with pre-chilled PBS buffer and then incubated with pH 2.5 buffer (0.5 M NaCl, 0.5 M acetic acid) for 5 min on ice to remove surface transferrin. Finally, the cells were washed with PBS buffer twice and solubilized with 0.1 N NaOH and transferred to tubes suitable for γ-counting. Each timepoint was treated individually. For the steady-state surface transferrin measurement, the plate was incubated at 4℃ for 2 h instead of 37℃ and then washed with PBS buffer six times and solubilized for γ-counting. The specific radioactivity of intracellular and surface transferrin was calculated by subtracting the radioactivity in the competition well from the average radioactivity of the triplicate wells. The kinetics of transferrin internalization was analyzed by plotting the ratio of internal transferrin to surface transferrin ratio as a function of time.

Measurement of kinetics of transferrin receptor recycling

Cells were seeded into 6-well plates one day before the experiment, as described previously for the internalization assay. On the day of the experiment, the cells in the triplicate and competition wells were loaded with radioactive transferrin, as described above, for 1 h at 37℃. Plates were removed at various times and washed with pre-warmed (37℃) serum-free medium and then incubated with pre-warmed pH 4.6 buffer (150 mM NaCl, 1 mM $CaCl_2$, 20 mM sodium acetate buffer) for 2 min. The cells were then washed with pre-warmed efflux medium (serum-free medium with 0.2% BSA, 20 mM HEPES (pH 7.2), 100 µg/ml human transferrin) three times over the course of 1 min. The plate was fed with 1 ml of efflux medium and incubated for the indicated times (2, 5, 10, 20, 40, 60 min) to allow recycling of internalized transferrin. At different time points, the efflux medium was transferred into a tube for γ-counting. Another 1 ml of efflux medium was added to the cells as a wash and transferred to the tube for γ-counting. The cells were solubilized and transferred to tubes to determine the radioactivity of the internalized transferrin. Transferrin receptor recycling was defined by the ratio between the radioactivity of transferrin in the medium and total transferrin (transferrin in medium and internalized transferrin).

Treatment of MEF cells with agents that elevate vesicular pH

Reconstituted and knockout cells were treated with 2 µM monensin (M5273), 25 µM chloroquine (C6628), 10 nM bafilomycin A1 (B1793) (Sigma-Aldrich) or 5 µg/ml brefeldin A (Biolegend) for 16 h followed by fluorescence activated cell sorting analysis.

Cholix toxin treatment of MEF cells

Reconstituted and knockout cells were seeded (3×10^4) into wells of a 96-well plate and treated with 0.5 µg/ml cholix toxin for 48 h and 72 h. An MTS assay (Promega) was used to measure cell viability according to the manufacturer's instructions.

LDL internalization assay

Reconstituted and knockout cells were seeded onto 12-well plates with coverslips and incubated overnight. The next day, the cells were serum-starved for 2 h and incubated with Alexa-488-conjugated LDL-containing serum-free medium for 1 h and chased with serum-free medium for various times.

Flow cytometry

Reconstituted and knockout cells were detached by treatment with PBS-EDTA. Cells (1×10^5) were then incubated with FITC-conjugated antibodies against TRFC1 and integrin α5 or an isotope-matched control antibody for 1 h to visualize cell surface expression or were permeabilized using permeabilization solution (BD Biosciences) and then incubated with the above antibodies to visualize both internal and surface expression. Afterwards, the cells were washed with PBS twice and analyzed by using flow cytometry (FACSCalibur, BD Biosciences). Data were analyzed with Cell Quest Pro software or FlowJo.

Immunoblot analysis

Total cell lysates from transfected 293ETN or MEF cells were obtained by incubating the cells in standard lysis buffer (50 mM Tris-HCl, pH 8, 150 mM NaCl, 5 mM EDTA, pH 8, 1% NP-40) containing a protease inhibitor cocktail (Roche). Cytoplasmic and membrane fractions were extracted by sequentially lysing cells in HE buffer (0.02% digitonin, 50 mM HEPES, pH 7.5, 150 mM NaCl, 2 mM $CaCl_2$, 10 mM N-ethyl maleimide and protease inhibitors) and lysis buffer (10 mM Tris, pH 7.4, 100 mM NaCl, 1 mM EDTA, 1 mM EGTA, 1% Triton X-100, 10% glycerol, 0.1% SDS, 0.5% deoxycholate and protease inhibitors). Protein was quantified using the Bradford method and subjected to SDS-PAGE. Proteins were transferred to PVDF membranes (Millipore). Membranes were blocked with Odyssey blocking buffer (LI-COR Biosciences), incubated with rabbit polyclonal antibodies against LRP1 or TFRC2 and a mouse monoclonal against β-actin at 4℃ overnight and washed with TBS buffer with 0.2% Tween-20. After incubation with infrared secondary IRDye 800 and IRDye 680 anti-rabbit or anti-mouse IgG (1 in 15,000, LI-COR Biosciences), membranes were scanned using an Odyssey Infrared Imaging System. Band sizing was performed using Odyssey 3.0 software (LI-COR Biosciences) and quantification of LRP1was performed by normalizing the specific probe band intensity to that of β-actin.

Surface protein analysis

Cell surface proteins were biotinylated using the membrane-impermeable reagents sulfo-NHS-LC-biotin and sulfo-NHS-SS-biotin (1 mg/ml) (Pierce), according to the manufacturer's instructions. Equal amounts of cellular protein from reconstituted and knockout MEF cells were incubated with streptavidin–agarose overnight at 4℃ and washed three times. The proteins were eluted with SDS sample buffer for SDS-PAGE and immunoblot analysis.

Stable isotope labeling by amino acids in cell culture protein quantification

Stable isotope labeling by amino acids in cell culture (SILAC) was performed by seeding and growing equal numbers of reconstituted and knockout cells in medium containing heavy (^{13}C, ^{15}N) and light isotopes (^{12}C, ^{14}N) (Pierce), respectively. Three-day culture media were collected and concentrated through a 10-kDa molecular weight cutoff Amicon filtration system. The secreted protein mixtures were separated in a 4–12% SDS-PAGE gel and stained with Coomassie Brilliant Blue. The differentially expressed protein bands were excised and analyzed by liquid chromatography tandem mass spectrometry (LC-MS/MS) at the Taplin Biological Mass Spectrometry Facility of Harvard University.

Proteomics and co-immunoprecipitation

Lysates from reconstituted and knockout cells were prepared as described for immunoblotting analysis. They were incubated with anti-Flag beads (Sigma-Aldrich) for 4 h at 4℃. After washing with cell lysis buffer with salt three times, the binding proteins were eluted by using Flag peptide. The eluted proteins were separated in a 4–12% SDS-PAGE gel and stained with Coomassie Brilliant Blue. The gel was sliced in several sections and sent for mass spectrometry analysis. For co-immunoprecipitation assay, the cell lysates from MEF cells or transfected 293ETN cells were incubated with the corresponding antibodies and then adsorbed on protein A/G beads. After washing, the bound proteins were eluted in SDS sample loading buffer. The immunoblotting procedure described above was followed to identify candidate interacting proteins.

Statistical analyses

Student's *t*-test was used to determine the statistical significance of differences between groups.

Acknowledgements

We thank Naifang Lu for microinjection of embryonic stem cells, Huajun Wang for sequence data analysis and Zhifang Cao for help with proteomics (all affiliated with Massachusetts General Hospital, MA).

Competing interests

The authors declare no competing interests.

Author contributions

Guo Ling Zhou conceived, designed and executed experiments, interpreted data and prepared the article. Soon-Young Na interpreted data and prepared the article. Rasma Niedra performed experiments. Brian Seed designed experiments, interpreted data and prepared the article.

Funding

This work was supported by Massachusetts General Hospital.

Supplementary material

Supplementary material available online at
http://jcs.biologists.org/lookup/suppl/doi:10.1242/jcs.135269/-/DC1

References

Arai, K. Y. and Nishiyama, T. (2007). Developmental changes in extracellular matrix messenger RNAs in the mouse placenta during the second half of pregnancy: possible factors involved in the regulation of placental extracellular matrix expression. *Biol. Reprod.* **77**, 923-933.

Assémat, E., Vinot, S., Gofflot, F., Linsel-Nitschke, P., Illien, F., Châtelet, F., Verroust, P., Louvet-Vallée, S., Rinninger, F. and Kozyraki, R. (2005). Expression and role of cubilin in the internalization of nutrients during the peri-implantation development of the rodent embryo. *Biol. Reprod.* **72**, 1079-1086.

Carter, M. G., Sharov, A. A., VanBuren, V., Dudekula, D. B., Carmack, C. E., Nelson, C. and Ko, M. S. (2005). Transcript copy number estimation using a mouse whole-genome oligonucleotide microarray. *Genome Biol.* **6**, R61.

Christensen, E. I. and Birn, H. (2002). Megalin and cubilin: multifunctional endocytic receptors. *Nat. Rev. Mol. Cell Biol.* **3**, 256-266.

Christensen, E. I. and Verroust, P. J. (2002). Megalin and cubilin, role in proximal tubule function and during development. *Pediatr. Nephrol.* **17**, 993-999.

Edgar, A. J. (2007). Human GPR107 and murine Gpr108 are members of the LUSTR family of proteins found in both plants and animals, having similar topology to G-protein coupled receptors. *DNA Seq.* **18**, 235-241.

Elling, U., Taubenschmid, J., Wirnsberger, G., O'Malley, R., Demers, S. P., Vanhaelen, Q., Shukalyuk, A. I., Schmauss, G., Schramek, D., Schnuetgen, F. et al. (2011). Forward and reverse genetics through derivation of haploid mouse embryonic stem cells. *Cell Stem Cell* **9**, 563-574.

Fisher, C. E. and Howie, S. E. (2006). The role of megalin (LRP-2/Gp330) during development. *Dev. Biol.* **296**, 279-297.

Goossens, K., Van Soom, A., Van Zeveren, A., Favoreel, H. and Peelman, L. J. (2009). Quantification of fibronectin 1 (FN1) splice variants, including two novel ones, and analysis of integrins as candidate FN1 receptors in bovine preimplantation embryos. *BMC Dev. Biol.* **9**, 1.

Harrison, S. C. and Kirchhausen, T. (2010). Structural biology: Conservation in vesicle coats. *Nature* **466**, 1048-1049.

Herz, J. and Strickland, D. K. (2001). LRP: a multifunctional scavenger and signaling receptor. *J. Clin. Invest.* **108**, 779-784.

Iwaki, T., Sandoval-Cooper, M. J., Paiva, M., Kobayashi, T., Ploplis, V. A. and Castellino, F. J. (2002). Fibrinogen stabilizes placental-maternal attachment during embryonic development in the mouse. *Am. J. Pathol.* **160**, 1021-1034.

Jørgensen, R., Purdy, A. E., Fieldhouse, R. J., Kimber, M. S., Bartlett, D. H. and Merrill, A. R. (2008). Cholix toxin, a novel ADP-ribosylating factor from Vibrio cholerae. *J. Biol. Chem.* **283**, 10671-10678.
Kaseda, R., Hosojima, M., Sato, H. and Saito, A. (2011). Role of megalin and cubilin in the metabolism of vitamin D(3). *Ther. Apher. Dial.* **15 Suppl. 1**, 14-17.
Kozyraki, R. and Gofflot, F. (2007). Multiligand endocytosis and congenital defects: roles of cubilin, megalin and amnionless. *Curr. Pharm. Des.* **13**, 3038-3046.
Kozyraki, R., Fyfe, J., Kristiansen, M., Gerdes, C., Jacobsen, C., Cui, S., Christensen, E. I., Aminoff, M., de la Chapelle, A., Krahe, R. et al. (1999). The intrinsic factor-vitamin B12 receptor, cubilin, is a high-affinity apolipoprotein A-I receptor facilitating endocytosis of high-density lipoprotein. *Nat. Med.* **5**, 656-661.
Kozyraki, R., Fyfe, J., Verroust, P. J., Jacobsen, C., Dautry-Varsat, A., Gburek, J., Willnow, T. E., Christensen, E. I. and Moestrup, S. K. (2001). Megalin-dependent cubilin-mediated endocytosis is a major pathway for the apical uptake of transferrin in polarized epithelia. *Proc. Natl. Acad. Sci. USA* **98**, 12491-12496.
Langerak, P., Nygren, A. O., Schouten, J. P. and Jacobs, H. (2005). Rapid and quantitative detection of homologous and non-homologous recombination events using three oligonucleotide MLPA. *Nucleic Acids Res.* **33**, e188.
Lewis, M. J. and Pelham, H. R. (1990). A human homologue of the yeast HDEL receptor. *Nature* **348**, 162-163.
Majoul, I., Straub, M., Hell, S. W., Duden, R. and Söling, H. D. (2001). KDEL-cargo regulates interactions between proteins involved in COPI vesicle traffic: measurements in living cells using FRET. *Dev. Cell* **1**, 139-153.
Marsh, M. and McMahon, H. T. (1999). The structural era of endocytosis. *Science* **285**, 215-220.
Nykjaer, A., Fyfe, J. C., Kozyraki, R., Leheste, J. R., Jacobsen, C., Nielsen, M. S., Verroust, P. J., Aminoff, M., de la Chapelle, A., Moestrup, S. K. et al. (2001). Cubilin dysfunction causes abnormal metabolism of the steroid hormone 25(OH) vitamin D(3). *Proc. Natl. Acad. Sci. USA* **98**, 13895-13900.
Pelham, H. R. (1991). Recycling of proteins between the endoplasmic reticulum and Golgi complex. *Curr. Opin. Cell Biol.* **3**, 585-591.
Pfeffer, S. R. (2001). Membrane transport: retromer to the rescue. *Curr. Biol.* **11**, R109-111.
Pucadyil, T. J. and Schmid, S. L. (2009). Conserved functions of membrane active GTPases in coated vesicle formation. *Science (New York, N.Y.)* **325**, 1217-1220. doi: 10.1126/science.1171004.
Seaman, M. N. (2005). Recycle your receptors with retromer. *Trends Cell Biol.* **15**, 68-75.
Wassmer, T., Attar, N., Bujny, M. V., Oakley, J., Traer, C. J. and Cullen, P. J. (2007). A loss-of-function screen reveals SNX5 and SNX6 as potential components of the mammalian retromer. *J. Cell Sci.* **120**, 45-54.
Willnow, T. E., Nykjaer, A. and Herz, J. (1999). Lipoprotein receptors: new roles for ancient proteins. *Nat. Cell Biol.* **1**, E157-E162.
Wolfe, B. L. and Trejo, J. (2007). Clathrin-dependent mechanisms of G protein-coupled receptor endocytosis. *Traffic* **8**, 462-470.
Yang, Y. and Seed, B. (2003). Site-specific gene targeting in mouse embryonic stem cells with intact bacterial artificial chromosomes. *Nat. Biotechnol.* **21**, 447-451.